

# Modeling of radiation heat transfer in the dense-bed flow of solid pyrolysis in indirectly heated rotary kilns

S. Tavakkol\*<sup>1</sup>, T. Zirwes<sup>2,3</sup>, J.A. Denev<sup>2</sup>, H. Bockhorn<sup>3</sup>, D. Stapf<sup>1</sup>

\*Salar.Tavakkol@kit.edu

<sup>1</sup> Karlsruhe Institute of Technology, Institute of Technical Chemistry, Eggenstein-Leopoldshafen

<sup>2</sup> Karlsruhe Institute of Technology, Steinbuch Centre for Computing, Eggenstein-Leopoldshafen

<sup>3</sup> Karlsruhe Institute of Technology, Engler-Bunte-Institute, Karlsruhe

## Abstract

This work presents the further development and the validation of the Discrete Ordinates Model for thermal radiation which is implemented in OpenFOAM® for application to packed beds of biomass particles. This radiation model is an important part of a more comprehensive model which simulates the thermal conversion of discrete phase (here for instance wet biomass particles) which flows continuously inside an indirectly heated rotary kiln. The comprehensive Eulerian-Lagrangian model integrates three-dimensional, time-resolved simulation of the essential chemical and physical processes occurring within and in-between the moving bed of particles. This is realized by combining the particle collision models for non-reactive dense flows with models for heat transport, phase change and chemical reaction for multiphase reacting flow in the framework of OpenFOAM®.

For the thermal treatment of solid particles, convection and radiation heat transfer methods couple the energy exchange between the reactor wall, gas- and disperse phase. The original implementation of the finite volume Discrete Ordinate Model (fvDOM) valid for a dilute particulate phase neglects the effect of local opacity due to the existence of individual particles. However, in the present application, a dense-packed bed of the particulate phase exists in the reactor. Therefore, in this study, this direction-based radiation model is adjusted for a computational cell with arbitrary particle volume fractions.

To validate the results with the present thermal radiation model, first a simple test case with heating the bed of particles from the top of the domain is carried out. A second test relates to a laboratory-scale reactor. The results of the improved fvDOM are compared to the original implementation of OpenFOAM® and the more simple and computationally cheap P-1 radiation model. In general, the P-1 model largely overpredicts the radiative heat transfer while the original fvDOM underpredicts the heat flux by about 15% for the first test case. The improved model delivers results within 1% deviation at the expense of maximum 10% of the increase in the computational time.

## Introduction

The thermochemical conversion of biomass is governed by a large number of concurrent physical and chemical processes. They include the motion of the pieces of biomass (from here on referred to as particles) their heating-up, drying, shrinkage and the primary pyrolysis involving a very large number of chemical reactions. It is therefore complex to investigate [1]–[6] and the detailed modeling often requires the use of supercomputers [7]–[10]. One parameter of major importance for this process is the heat transferred to the packed bed of solid particles by conduction, convection and radiation. In [7] we presented details about the utilized Eulerian-Lagrangian approach and performed validations with both laboratory and industrial-scale rotary kiln reactors. Further details of the developed model are presented in [11].

Classical models of computational fluid dynamics (CFD) have been developed for coal combustion or fine sprays applications. Therefore, they assume that particles occupy a small volume of the computational cell and are diluted in the gas phase. However, the presence of a packed bed of particles residing at the bottom of the reactor requires special treatment and further developments in each part of the modeling. The present study deals with the developments related to radiative heat transfer in packed beds. It describes how the shadowing effect between particles of the bed is accounted for. The improvements are tested against different radiation models from the literature. Therefore, in the following, a short literature review of the models that handle radiative heat transfer of biomass is presented and their specific strengths and limitations are highlighted.

The lowest-order spherical harmonic method, P-1 is a radiation model suitable for high and homogenous optical thickness and has been used in many research studies and proved to be an acceptable model when it comes to applications, where the dense bed of solid particles is not formed, i.e. homogenous scattering exists [12]–[16]. The P-1 model has the advantage that it easily applies to complicated geometries [17]. Its popularity originates from the fact that it solves a partial differential

equation for the incident radiation which uses the same numerical methods as the other transport equations and is hence easy to solve, but in optically thin media its accuracy can decrease [13], [18]. The equation solved is of a diffusion nature with a proportionality constant that is a single scalar variable and therefore the model cannot handle directional inhomogeneities.

Ku et al. [14] used the P-1 model for gasification of biomass in fluidized bed reactor stating that it has generally been chosen in CFD simulations of pulverized fuel gasification with radiation scattering. Their particle model has been of the Lagrangian type and temperatures in the reactor were up to 920 °C. Liu et al. [16] applied the P-1 model successfully in a 3D steady-state CFD model to simulate biomass gasification in a circulating fluidized-bed reactor with gas temperatures reaching up to 1000 °C. The results showed that the impact of thermal radiation was significant and that thermal radiation needs to be included in the gasification model, however, there was no comparison with measured temperatures in this study. This study used the Eulerian-Eulerian approach.

Klason et al. [13] concluded that the radiative heat transfer rates to the fuel bed are sensitive to the different radiative heat transfer models. For a realistic presentation of the radiative heat transfer to/from the particle bed they suggested applying more computationally demanding models like the grey gas model based on the finite volume discretization (FGG) or, the spectral line weighted-sum-of-grey-gases model (SLW) which, in their study was also based on finite volumes. The temperature distribution in the furnace obtained with the P-1 model was similar to the other models. However, the trend of the radiative heat flux to the fuel bed was not realistically captured by the P-1 model which predicted a net heat transfer from the bed to the free-room of the large-scale industry furnace.

Gomez et al. [19] noticed that numerical codes are mature for the simulation of the gas phase but need to be further developed to accommodate also the processes in the solid phase. In their study of the biomass combustion with packed beds, they consider the packed bed as a porous medium and modified the original Discrete Ordinate Model (DOM) so that it can account for the temperature difference between the solid and gas phases and the high absorptivity of the medium. Khodaei et al. [20] applied the DOM modification proposed by [19] with the motivation that it can overcome the energy imbalance associated with the standard DOM.

[21] used the DOM together with the weighted sum of grey gases for biomass combustion in the packed bed with a comprehensive validation of multiphysics modeling. They improved the DOM to account for the radiative heat transfer between the particles, the particles and the walls as well as the radiation from the freeboard above the packed bed. The model requires summation over temperatures of neighbor particles within a spherical volume which in general, could turn to be computationally very intensive.

The above-cited papers for the DOM use commercial codes for their studies. In the present paper, we apply the open-source code OpenFOAM® to study and validate the radiative part of a generally very comprehensive model for thermal conversion of biomass in rotary kiln reactors. The current study applies and compares three models for the radiative heat transfer: the P-1 model, the standard DOM as well as the present implementation, i.e. improved model, accounting for the shadowing effect between neighboring particles.

## Modeling approach

### Governing equations

The flow of the continuous phase is described by the fully compressible Navier-Stokes equations and numerically solved by using the finite volume method (FVM) within the framework of OpenFOAM [22]. In addition, the balance equations for energy and chemical species masses are included as well. Since the focus of this work lies in the modeling of the discrete phase, the reader is referred to [11] for an overview of the numerical description of the continuous phase.

Each biomass particle in the simulation is modeled in a Lagrangian frame of reference. The particles' movement is therefore described by Newton's law, as shown in Eq. 1 considering the external forces  $\mathbf{F}$  acting on the biomass particles:

$$m_p \frac{d\mathbf{v}_p}{dt} = \sum \mathbf{F}_{\text{external}} = \mathbf{F}_c + \mathbf{F}_g + \mathbf{F}_d + \mathbf{F}_p + \mathbf{F}_v, \quad \text{Eq. 1}$$

where  $\mathbf{v}_p$  is the velocity of particle  $p$  and  $m_p$  its mass. For the forces, collisions between particles or between a particle and the reactor wall ( $\mathbf{F}_c$ ) are taken into account as well as gravity ( $\mathbf{F}_g$ ) and the drag force assuming solid spheres ( $\mathbf{F}_d$ ). Forces due to pressure gradients are neglected [23]. With Eq. 1, the particles' position  $x_p$  is then determined from

$$\frac{dx_p}{dt} = \mathbf{v}_p \quad \text{Eq. 2}$$

When the wet biomass particles enter the kiln, different physico-chemical processes occur. This entails drying and devolatilization, which leads to a reduction of the particle mass over time. Because of this, the change of particle mass has to be included in the numerical description as well:

$$-\frac{dm_p}{dt} = \frac{dm_{\text{drying}}}{dt} + \frac{dm_{\text{devolatilization}}}{dt} \quad \text{Eq. 3}$$

The composition of the biomass particles in the numerical model considers moisture, char, ash and volatiles (tar, water, carbon monoxide and carbon dioxide). During the drying phase, moisture is converted from the discrete phase to water vapor and added to the continuous phase. This process is described by a combined model that considers thermal drying and a linearized diffusion-based model [7]. Likewise, during devolatilization, the volatile species are transferred from the discrete particles to the continuous gas phase. For this, a kinetic model based on experimental measurements is employed [24], [25]. Once the biomass particles are dried and the devolatilization process has finished, the particles finally consist of ash and char with no further reactions occurring. For a more detailed description of the devolatilization and drying models, see [11].

The change in particle mass due to drying and devolatilization also yields in the change of the particle diameter  $d_p$ . In this work, a constant particle density  $\rho_p$  is assumed, so that the particle diameter can be computed from:

$$d_p = \left( \frac{6 m_p}{\pi \rho_p} \right)^{1/3}, \quad \text{Eq. 4}$$

Lastly, to describe the temperature of the biomass particles  $T_p$ , an energy balance equation for each Lagrangian particle is solved:

$$m_p c_{p_p} \frac{dT_p}{dt} = -\dot{Q}_{\text{drying}} - \dot{Q}_{\text{devolatilization}} + \dot{Q}_{\text{convection}} + \dot{Q}_{\text{radiation}} \quad \text{Eq. 5}$$

$\dot{Q}_{\text{drying}}$  is the energy required for the phase change of the water,  $\dot{Q}_{\text{devolatilization}}$  is caused by the endothermic devolatilization process and  $c_{p_p}$  is the isobaric heat capacity of the particle, which is a function of the temperature and current particle composition.  $\dot{Q}_{\text{convection}}$  and  $\dot{Q}_{\text{radiation}}$  describe the heat transfer due to convection and radiation, which are described in more detail in the following subsection.

#### Heat transfer model: convective heat transfer

The accurate modeling of convective heat transfer plays an important role because the particles are assumed to be perfect spheres and therefore do not conduct heat due to direct contact.

A correlation based on the Nusselt number  $Nu$  is employed to express the convective heat transfer from Eq. 5 as

$$\dot{Q}_{\text{convection}} = Nu \cdot \pi \cdot \lambda_g \cdot d_p \cdot (T_g - T_p), \quad \text{Eq. 6}$$

where  $\lambda_g$  is the thermal conductivity of the continuous gas phase gas mixture and  $T_g$  its temperature. The Nusselt number itself is defined as

$$Nu = \frac{h_p \cdot d_p}{\lambda_g}, \quad \text{Eq. 7}$$

where  $h_p$  is the heat transfer coefficient. Due to the generally low gas velocities in the kiln, the Ranz-Marshall model is used to compute the Nusselt number assuming particulate flow with Reynolds numbers less than  $5 \times 10^4$  [26]:

$$Nu = 2 + 0.6 \cdot Re_p^{1/2} \cdot Pr^{1/3}, \quad \text{Eq. 8}$$

$Re_p$  is the particle Reynolds number and  $Pr$  the Prandtl number.

#### Heat transfer model: radiative heat transfer

While the heat transfer due to convection, as described above, is already available in OpenFOAM, there is no accurate description of heat transfer by radiation for dense particle beds. More specifically, the available models do not consider that the particles have a non-zero diameter and therefore shield each other from radiation. To overcome this, the finite volume discrete ordinates model (fvDOM) has been extended in this work to take into account the effect of dense particle beds on radiative heat transfer.

The radiative heat transfer to particles from Eq. 5 is formulated as

$$\dot{Q}_{\text{radiation}} = \epsilon_p A_s \left( \frac{1}{4} \int_{4\pi} I d\Omega - \sigma T_p^4 \right), \quad \text{Eq. 9}$$

where  $\epsilon_p$  is the particle's emissivity by the overall agreement from experimental work obtained for particles  $\epsilon_p = 0.70$  and for the wall  $\epsilon_w = 0.85$  [11].  $A_s$  is the projected area of the particle and  $\sigma$  the Stefan-Boltzmann constant. The radiation intensity  $I$  is obtained by integration over all directions. The change of the radiation intensity along a path  $ds$  is given by the Radiative Transport Equation (RTE)

$$\frac{dI}{ds} = \kappa I_b - \kappa I. \quad \text{Eq. 10}$$

The right-hand side of Eq. 10 describes the change of radiation intensity due to absorption with the absorption coefficient  $\kappa$  and  $I_b$  is the black body radiation. Discretizing Eq. 10 in the space leads to the following equation for each discrete direction in a cell. To solve Eq. 11 numerically, the finite volume discrete ordinates model (fvDOM) is used in OpenFOAM.

$$\frac{1}{V} \sum_i^N \sum_k I_{k_i} (S_i \cdot \hat{n}_k) A_k = -\kappa_{\text{total}} I_{V_i} \Omega_i + \Omega_i \left( \kappa_g I_{\text{bpg}} + \frac{E_{\text{disperse}}}{4\pi} \right)_V \quad \text{Eq. 11}$$

The term on the left side represents the sum of values (in this study: rays) on the cell surfaces indexed with  $k$ .  $S_i$  is the location variable in the direction of the ray  $i$ ,  $\hat{n}_k$  and  $A$  are the normal vector and the surface area of the corresponding surface, respectively. The sums express the total amount of incoming radiation from all directions to the specified cell  $V$ . The right-hand side of Eq. 11 consists of two terms; one for absorption and another for emission.  $\Omega_i$  are the discrete directions with solid angles, the former expresses the total absorption of the cell with cell's absorption/emission coefficient  $\kappa_{\text{total}}$  and the latter represents the emission which is divided into two parts for the continuous and dispersed phases. So, in order to determine the radiation delivered to each particle, Eq. 9 has to be calculated for which Eq. 11, the numerical solution of Eq. 10 has to be solved. For that, the modified absorption/emission coefficient and emission intensity to consider densely packed particles are modified and introduced in the following equations in the next section.

#### Modifications to fvDOM model

The fvDOM model is valid to calculate the absorption/emission coefficient and emission intensity for the dispersed phase, only if the particle volume fraction is low or in other words, the sum of the projected area of particles is much smaller than the cell surface. The highlighted restriction in 3D models is that the shading effect in the direction-dependent projected area of particles cannot be considered in control volumes. Therefore, by highly packed cells, the sum of the projected surface of spheres can exceed the real projected area of the cell.

A modification for the determination of the absorption/emission coefficient for the dense disperse flows is developed and implemented in OpenFOAM®. In this method, the ratio of the cell projected surface to the projected area of all particles within that cell is considered for any arbitrary ray direction  $\Omega_i$ .

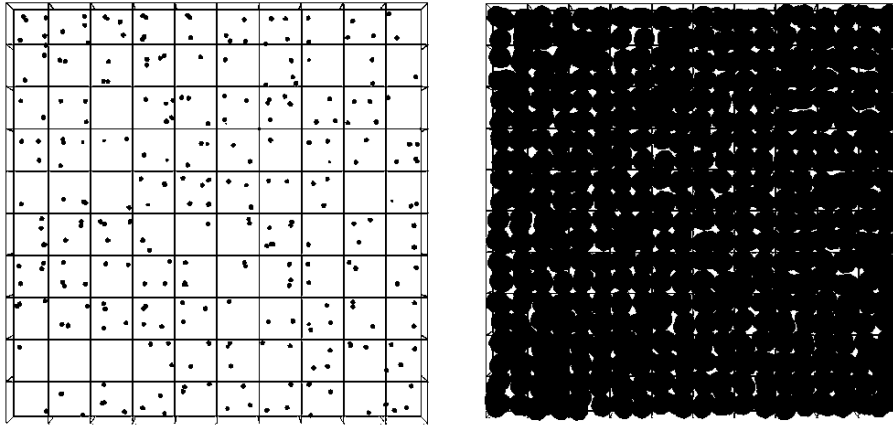


**Figure 1** Comparison of cells' area (in white) and particles' projected area (dark) in the low and high particle volume fraction in cells.

The left-hand side image in Figure 1 represents a case study with a low ratio of the particles-to-cell projected area where the default equations of OpenFOAM® for absorption/emission coefficient and emission intensity are valid. The image in the right-hand frame of Figure 1 shows an example case of fully packed particles in multilayers consecutively, in which the sum of the projected area of particles is larger than the cell projected area.

A modification for equations related to the  $\kappa_p$  absorption/emission coefficient and radiative emission  $E_{\text{disperse}}$  is suggested to use the minimum and maximum functions in order to return a value with the smaller and larger quantities from the two arguments, respectively.

The calculation of  $\kappa_p$  and  $E_{\text{disperse}}$  should fulfill both usual possibilities related to the projected area of a cell and its containing particles:

- cells with low particle volume fraction, where  $\sum_{i=1}^{n_{\text{pcell}}} A_{p_i} < A_{\text{pc}}$ ,
- cells with high particle volume fraction, where  $\sum_{i=1}^{n_{\text{pcell}}} A_{p_i} \geq A_{\text{pc}}$ .

$n_{\text{pcell}}$  is the number of particles in the corresponding computational cell,  $A_{\text{pc}}$  is the direction-dependent projected area of the cell and  $A_{p_i}$  declares the projected area of each spherical particle by  $A_{p_i} = \frac{\pi d_{p_i}^2}{4}$ . The modified equation of the absorption/emission coefficient uses the minimum and maximum functions to return a value with the smaller and larger quantities from the two arguments, respectively.

$$\kappa_p = \frac{A_{\text{pc}}}{V} \frac{\min(A_{\text{pc}}, \sum A_{p_i})}{\max\{(A_{\text{pc}} - \sum A_{p_i}), A_{\text{small}}\}} \epsilon_p \quad \text{Eq. 12}$$

The min function in the nominator is responsible for the overlapping effect of particle projected area and ensures that the maximum limit of surface projection (cell projected surface) is not exceeded. This function applies the physical interpretation of shadowing and keeps the intensity balance of cells. The max function in the denominator, on the other hand, ensures the numerical stability and the correct sign of the absorption/emission coefficient for the circumstance of dense/packed disperse phase. The function prevents division by zero or negative values for  $\kappa_p$  through  $A_{\text{small}}$  as a constant small value. A good compromise between accuracy and numerical stability is found by the value of  $A_{\text{small}} = 2.5 \times 10^{-4} A_{\text{pc}}$ . The physical interpretation of very large  $\kappa_p$  means entire absorption of the incoming radiation intensity.

A similar principle has to be applied for the modification of radiative emission from particles in cells.

$$E_{\text{disperse}} = \min\left(1, \frac{A_{\text{pc}}}{\sum A_{p_i}}\right) \cdot \sigma \frac{\epsilon_p}{V} \sum_{i=1}^{n_{\text{pcell}}} A_{s_i} T_{p_i}^4 \quad \text{Eq. 13}$$

The min function in Eq. 13 takes the shading effect of particles into account. As long as the sum of the projected area of particles is less than the cell surface, the function applies unity values and acts neutrally. If the cell is densely packed, the ratio  $\frac{A_{\text{pc}}}{\sum A_{p_i}}$  can be smaller than one and therefore the function applies a factor less than one to fulfill the shading effect of the total emission. The factor basically considers a part of the emission that finds no way to leave the cell and is absorbed by neighboring particles.

### Overview of numerical methods

The presented solver in this work is based on the described coupling and developed submodels from the previous work of authors [7], [11], [27], [28]. A simplified numerical scheme of the developed solver during one timestep is shown in Figure 2. Calculations for each phase are sketched in separate blocks. Mass, momentum and energy exchange between phases are handled through source terms. Regarding the discrete phase, for the particle collision the MP-PIC model is used which assumes that parcels are made up of uniform groupings of particles, where all share the same physical properties in each parcel (i.e. computational cluster). Further details regarding the particle collision model can be found in [11].

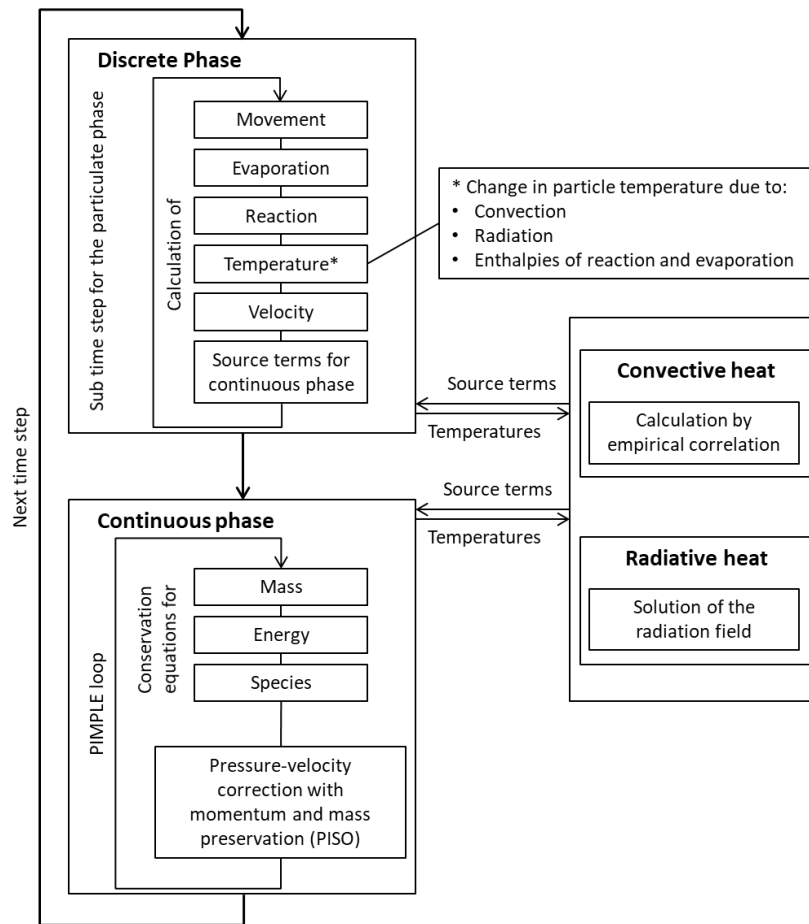


**Figure 2** Simplified numerical flowchart of the solver for one timestep.

### Validation of the Extended Radiation Model for Dense Particle Flows

The newly implemented improvement to OpenFOAM's fvDOM model for the consideration of dense particle flows is validated with two configurations. First, a simple test case is employed, where a box of side length 20 cm is filled with a bed of equally sized particles with 6 mm diameter, where no convection is considered (i.e. vacuum box). The particle diameter coincides with the computational cell size, which represents the limiting case of high particulate volume fractions. In total, 1800 particles with an initial temperature of 373 K are placed in the box and form a bed of several layers or a height of 2 cm. All sides of the box are walls with a temperature of 373 K. To evaluate the behavior of the new radiation model, the temperature of the top wall is set to 673 K. The setup is shown in Figure 3 on the left.

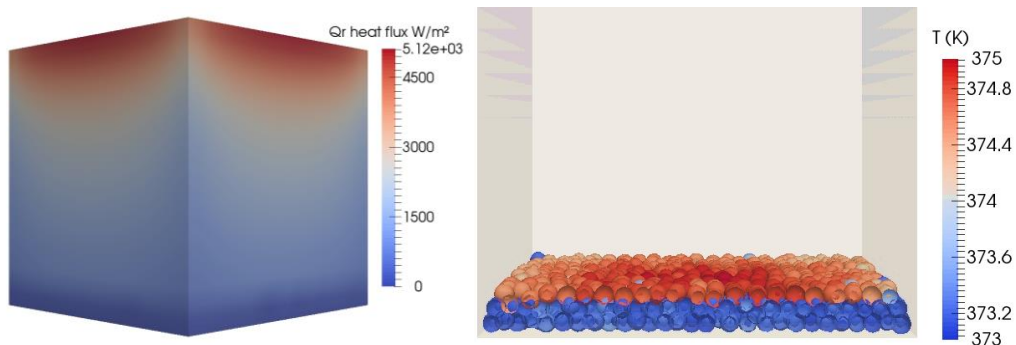


**Figure 3** Setup of the numerical test case. A box with hot top wall (left) is used to investigate the radiative heat transfer to bed particles (right).

When the simulation is started, the radiation from the top wall heats up the top layer of the particle bed, as shown in Figure 3 on the right. With the new implementation described in the previous section which takes the volume fraction of particles in the computational cells into account, the top layer shields the lower layers from the radiation of the top wall, so that only the top layer heats up.

The simulation is stopped after a physical time of 11 s. The total heat flow from the top wall to the particles can be determined by the increase of energy from all particles:

$$\dot{Q}_{p_{total}} = \dot{Q}_{radiation} = \frac{1}{\Delta t} \sum_i m_i c_{p_i} \Delta T_i \quad \text{Eq. 14}$$

where  $\dot{Q}_{p_{total}}$  is the total heat flow from the wall to the particles,  $\Delta t$  the simulation time and  $\Delta T_i$  the change of temperature of particle  $i$ .

Due to the simple setup, a view factor model can be used to estimate the expected heat flux. Assuming that the top particle layer can be described as a plane with the side length of 20 cm and a distance to the top wall of 18 cm yields a view factor between the top particle layer and the top wall of  $F_{1 \rightarrow 2} = 0.2286$ , calculated from [18]. With this, the heat flux based on the view factor methodology can be expressed as

$$\dot{Q}_{radiation} = \sigma F_{1 \rightarrow 2} 0.20^2 \text{ m}^2 (T_{top\ wall}^4 - T_{top\ layer}^4) \quad \text{Eq. 15}$$

where the  $T_{top\ wall}$  and  $T_{top\ layer}$  are the temperature of the upper wall and the initial temperature of the uppermost particle layer respectively.

**Table 1** Radiation heat flow in a box with 1800 particles: comparison of different models with view factor calculation.

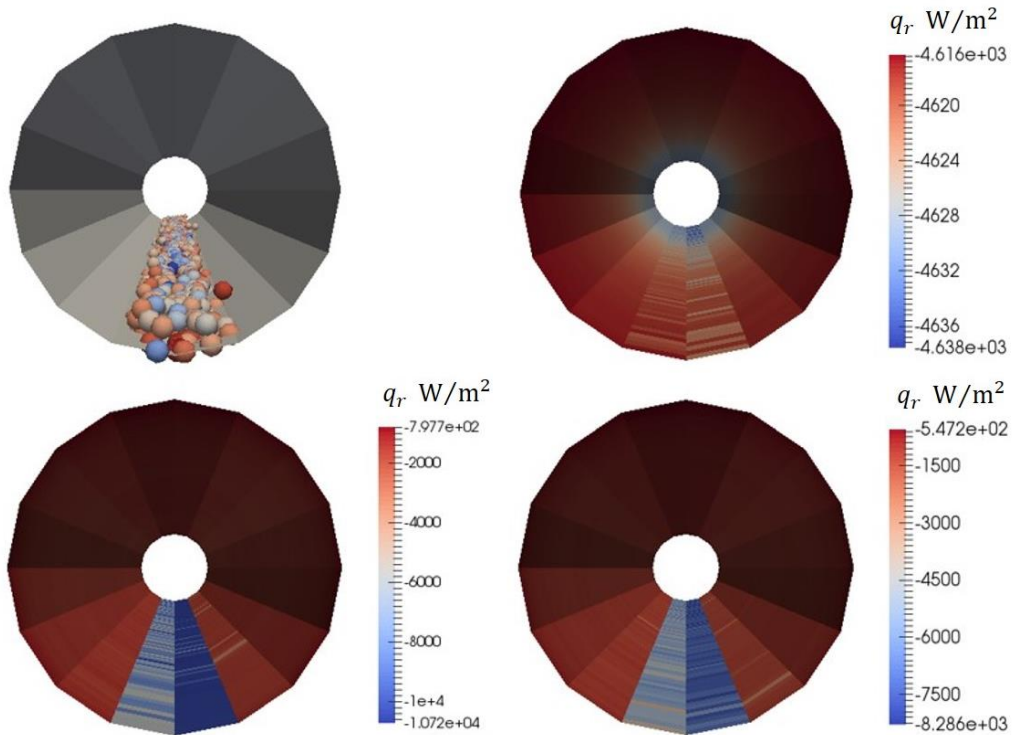
Heat flow (W)	View factor model	fvDOM (improved)	fvDOM	P-1
To particles	96.3	97.4	82.6	288.9
From all walls	96.3	96.7	82.4	289.5

Table 1 compares the estimated value of  $\dot{Q}_{radiation}$  from the view factor estimation in Eq. 15 with the simulation result from the improved fvDOM implementation. The new model yields excellent agreement within 1 % of the estimated heat flux. If the simulation is instead performed with OpenFOAM's original fvDOM model, which does not consider the shielding effect of the particles, the heat flow is underestimated by about 15 %. About 12.6 W of radiative heat flow reaches the bottom wall of the box when using standard fvModel, even though the bottom wall is fully covered by a dense particle bed. Even worse results are achieved by using the P-1 radiation model, which overestimates the heat flow by a factor of three. The reason is that the P-1 model is not well suited for cases where the optical thickness is not very high and where the distribution of radiation intensity is strongly anisotropic. As shown in Figure 4, the particle bed represents such an anisotropic case.

#### Validation of radiative heat transport in the rotating tube

A more complex test case is given by an experimentally investigated rotary kiln with a length of 1.4 m and an outer diameter of 8.5 cm by Carbolite Gero Ltd. (UK). The rotating tube is surrounded by an electric furnace, covering a length of 1 m. In the simulation, the same geometry as in the experimental setup is used. 1700 biomass particles with a diameter of 6 mm are inserted into the tube in the simulation and the tube walls are assumed to have a constant temperature of 673 K, while the biomass particles have an initial temperature of 320 K. The Simulation tests have been run for 11 seconds and the results from the last 10 seconds have been evaluated. In the large-scale setup, a realistic particle size distribution is defined up to 9 mm in diameter [7].

As in the previous test case of a particle bed in a box, the simulation of the particle bed in the kiln is performed with the improved fvDOM model, the standard fvDOM model and the P-1 radiation model. Figure 4 shows snapshots from the particle bed inside the kiln. On the top left, the position of the particles inside the reactor tube is shown. On the top right, the radiative heat flux at the kiln wall is shown for the simulation using the P-1 model. The radiative heat flux at the reactor walls from the improved fvDOM model is shown on the bottom left and the heat flux from the standard fvDOM model on the bottom right.



**Figure 4** Particle bed in the rotary kiln (top left), radiative heat flux  $q_r$  from the simulations using the P-1 model (top right), the improved fvDOM model (bottom left) and standard fvDOM model (bottom right).

The result from the P-1 model shows that the heat flux distribution is uniform in the circumferential direction. This means, that the P-1 model does not take the presence of the particles into account. For both the improved and original fvDOM model (bottom pictures in Figure 4), the presence of the particle bed has an influence on the predicted heat fluxes. For the simulation with the improved model, the heat flux from the bottom part of the kiln to the particle bed is about  $\dot{q}_r = -1.07 \times 10^4 \text{ W/m}^2$ , while for the original fvDOM model it is  $\dot{q}_r = -8.29 \times 10^3 \text{ W/m}^2$ . The expected heat flux can again be estimated, by considering the maximum possible heat flux (calculated with the temperature of the coldest particle) from the Stefan-Boltzmann law:

$$\dot{q}_{r,max} = \sigma(T_{wall}^4 - T_{p,min}^4) = 10949 \frac{\text{W}}{\text{m}^2} \quad \text{Eq. 16}$$

The comparison shows that the improved fvDOM model yields good agreement with this estimate, while the original fvDOM model underestimates the heat flux at this position by about 20 %.

**Table 2** Heat flow from the hot kiln walls to the particle bed from the simulation using the improved fvDOM model from this work, the standard fvDOM model and the P-1 model as well as computing time.

Model	$\dot{Q}$ (W)	computing time (s)
Improved fvDOM	930	2199
fvDOM	671	1990
P-1	1625	502

Table 2 summarizes the total heat flow from the kiln walls to the particle bed. Similar to the previous test case, the standard fvDOM model underestimates the heat flow to the particle bed, while the P-1 model overestimates it. In the kiln geometry, the difference between the original and improved fvDOM model is about 30 % and therewith much larger than in the simplified case of particles in a box, which highlights the need for accurate radiation modeling for more complex and realistic cases.

One critical aspect of radiation modeling is computational performance. The new fvDOM model for dense particulate flows requires additional computations based on the particle properties and distribution. Table 4 shows that the increase of simulation time is acceptable, with an overall increase of about 10 %. The simple P-1 model yields much faster simulation times, but with inadequate results. The computational efficiency of the model is an important factor since the final simulation in the large-scale model should run for 3000 seconds.

## Summary and Conclusions

Simulations of pyrolysis in rotary kilns is a challenging task due to many different physical processes governing the conversion of biomass to char. It requires the modeling of moisture evaporation to the gas phase, devolatilization as well as the interaction of biomass particles with each other in order to simulate the formation of particle beds. A new solver based on the open-source framework OpenFOAM has been developed that includes models for all relevant processes and allows to simulate the gas phase inside the kiln together with the particulate phase in a fully coupled manner. In industrial realizations of rotating heated kilns, heat transfer due to radiation plays an important role. Because of this, accurate radiation models are mandatory. However, commonly used radiation models are not formulated for dense particle flows and do not consider that particles from the particulate phase shield each other. In this work, an extension to the finite volume discrete ordinate model (fvDOM) has been developed that takes into account the volume fraction of the particulate phase in each computational cell and thus models the correct heat flux due to radiation to particle beds. A simple test case of a particle bed in a box with heated top wall shows the correct heating of only the top layer of the particle bed and yields a deviation of about 1 % from the expected heat flux. Without the new development, the heat flux is underestimated by 15 % and radiation from the top wall reaches the bottom wall, even though it is covered by large particles. The P-1 radiation model has shown to be inadequate due to the anisotropy introduced by the particle bed. The validation of the new model is completed with the application to a real kiln geometry by showing the improved modeling of radiative heat fluxes compared with the original fvDOM and P-1 models. The newly developed radiation model has therefore been shown to improve the predictive quality of biomass pyrolysis simulations in rotating kilns with acceptable computational overhead.

## References

- [1] C. Di Blasi, "Modeling chemical and physical processes of wood and biomass pyrolysis," *Prog. Energy Combust. Sci.*, vol. 34, no. 1, pp. 47–90, Feb. 2008, doi: 10.1016/j.pecs.2006.12.001.
- [2] W. C. Park, A. Atreya, and H. R. Baum, "Experimental and theoretical investigation of heat and mass transfer processes during wood pyrolysis," *Combust. Flame*, vol. 157, no. 3, pp. 481–494, Mar. 2010, doi: 10.1016/j.combustflame.2009.10.006.
- [3] A. Williams, M. Pourkashanian, and J. M. Jones, "Combustion of pulverised coal and biomass," *Prog. Energy Combust. Sci.*, vol. 27, no. 6, pp. 587–610, 2001, doi: 10.1016/S0360-1285(01)00004-1.
- [4] F. Wissing, S. Wirtz, and V. Scherer, "Simulating municipal solid waste incineration with a DEM/CFD method – Influences of waste properties, grate and furnace design," *Fuel*, vol. 206, pp. 638–656, Oct. 2017, doi: 10.1016/j.fuel.2017.06.037.
- [5] A. Sharma, V. Pareek, S. Wang, Z. Zhang, H. Yang, and D. Zhang, "A phenomenological model of the mechanisms of lignocellulosic biomass pyrolysis processes," *Comput. Chem. Eng.*, vol. 60, pp. 231–241, Jan. 2014, doi: 10.1016/j.compchemeng.2013.09.008.
- [6] A. Anca-Couce, "Reaction mechanisms and multi-scale modelling of lignocellulosic biomass pyrolysis," *Prog. Energy Combust. Sci.*, vol. 53, no. 2016, pp. 41–79, Mar. 2016, doi: 10.1016/j.pecs.2015.10.002.
- [7] S. Tavakkol *et al.*, "An Eulerian-Lagrangian method for wet biomass carbonization in rotary kiln reactors," *Renew. Sustain. Energy Rev.*, vol. 139, p. 110582, Apr. 2021, doi: 10.1016/j.rser.2020.110582.
- [8] W. Zhong, A. Yu, G. Zhou, J. Xie, and H. Zhang, "CFD simulation of dense particulate reaction system: Approaches, recent advances and applications," *Chem. Eng. Sci.*, vol. 140, pp. 16–43, 2016, doi: 10.1016/j.ces.2015.09.035.
- [9] H. P. Zhu, Z. Y. Zhou, R. Y. Yang, and A. B. Yu, "Discrete particle simulation of particulate systems: Theoretical developments," *Chem. Eng. Sci.*, vol. 62, no. 13, pp. 3378–3396, 2007, doi: 10.1016/j.ces.2006.12.089.
- [10] H. P. Zhu, Z. Y. Zhou, R. Y. Yang, and A. B. Yu, "Discrete particle simulation of particulate systems: A review of major applications and findings," *Chem. Eng. Sci.*, vol. 63, no. 23, pp. 5728–5770, 2008, doi: 10.1016/j.ces.2008.08.006.
- [11] S. Tavakkol, "Numerical Simulation of Wet Biomass Carbonization in Tubular Reactors," Karlsruhe Institute of Technology (KIT), PhD Thesis, 2021.
- [12] S. S. Sazhin, E. M. Sazhina, O. Faltsi-Saravelou, and P. Wild, "The p-1 model for thermal radiation transfer: Advantages and limitations," *Fuel*, vol. 75, no. 3, pp. 289–294, 1996, doi: 10.1016/0016-2361(95)00269-3.
- [13] T. Klason, X. S. Bai, M. Bahador, T. K. Nilsson, and B. Sundén, "Investigation of radiative heat transfer in fixed bed biomass furnaces," *Fuel*, vol. 87, no. 10–11, pp. 2141–2153, 2008, doi:

- 10.1016/j.fuel.2007.11.016.
- [14] X. Ku, T. Li, and T. Løvås, "CFD-DEM simulation of biomass gasification with steam in a fluidized bed reactor," *Chem. Eng. Sci.*, vol. 122, pp. 270–283, 2015, doi: 10.1016/j.ces.2014.08.045.
- [15] J. Xie, W. Zhong, Y. Shao, Q. Liu, L. Liu, and G. Liu, "Simulation of Combustion of Municipal Solid Waste and Coal in an Industrial-Scale Circulating Fluidized Bed Boiler," 2017, doi: 10.1021/acs.energyfuels.7b02693.
- [16] H. Liu, A. Elkamel, A. Lohi, and M. Biglari, "Computational fluid dynamics modeling of biomass gasification in circulating fluidized-bed reactor using the eulerian-eulerian approach," *Ind. Eng. Chem. Res.*, vol. 52, no. 51, pp. 18162–18174, 2013, doi: 10.1021/ie4024148.
- [17] R. I. Backreedy, L. M. Fletcher, L. Ma, M. Pourkashanian, and A. Williams, "Modelling pulverised coal combustion using a detailed coal combustion model," *Combust. Sci. Technol.*, vol. 178, no. 4, pp. 763–787, 2006, doi: 10.1080/00102200500248532.
- [18] M. F. Modest, *Radiative heat transfer*, Second ed. San Diego: Academic Press (Elsevier), 1993.
- [19] M. A. Gómez, J. Porteiro, D. Patiño, and J. L. Míguez, "CFD modelling of thermal conversion and packed bed compaction in biomass combustion," *Fuel*, vol. 117, no. PART A, pp. 716–732, 2014, doi: 10.1016/j.fuel.2013.08.078.
- [20] H. Khodaei, L. Gonzalez, S. Chapela, J. Porteiro, P. Nikrityuk, and C. Olson, "CFD-based coupled multiphase modeling of biochar production using a large-scale pyrolysis plant," *Energy*, vol. 217, p. 119325, 2021, doi: 10.1016/j.energy.2020.119325.
- [21] R. Mehrabian, A. Shiehnejadhesar, R. Scharler, and I. Obernberger, "Multi-physics modelling of packed bed biomass combustion," *Fuel*, vol. 122, no. 2014, pp. 164–178, 2014, doi: 10.1016/j.fuel.2014.01.027.
- [22] C. Greenshields and The OpenFOAM Foundation, "OpenFOAM User Guide," *OpenFOAM Foundation*, 2019. <https://cfd.direct/openfoam/user-guide/>.
- [23] C. T. Crowe, J. D. Schwarzkopf, M. Sommerfeld, and Y. Tsuji, *Multiphase with Droplets Flows and Particles*. CRC Press Taylor & Francis Group, 2012.
- [24] M. Müller-Hagedorn, H. Bockhorn, L. Krebs, and U. Müller, "A comparative kinetic study on the pyrolysis of three different wood species," *J. Anal. Appl. Pyrolysis*, vol. 68–69, pp. 231–249, 2003, doi: 10.1016/S0165-2370(03)00065-2.
- [25] M. Müller-Hagedorn and H. Bockhorn, "Pyrolytic behaviour of different biomasses (angiosperms) (maize plants, straws, and wood) in low temperature pyrolysis," *J. Anal. Appl. Pyrolysis*, vol. 79, no. 1-2 SPEC. ISS., pp. 136–146, 2007, doi: 10.1016/j.jaap.2006.12.008.
- [26] N. Wakao, S. Kagueli, and T. Funazkri, "Effect of fluid dispersion coefficients on particle-to-fluid heat transfer coefficients in packed beds. Correlation of Nusselt numbers," *Chem. Eng. Sci.*, vol. 34, no. 3, pp. 325–336, 1979, doi: 10.1016/0009-2509(79)85064-2.
- [27] S. Tavakkol, T. Zirwes, J. A. Denev, N. Weber, and H. Bockhorn, "Development and validation of an Euler-Lagrange method for the numerical simulation of wet-biomass carbonization in a rotary kiln reactor," *29. Dtsch. Flammentag*, 2019.
- [28] S. Tavakkol, T. Zirwes, J. A. Denev, F. Jamshidi, and H. Bockhorn, "Development of an Openfoam Solver for Numerical Simulation of Carbonization of Biomasses In Rotary Kilns," in *15th OpenFOAM Workshop*, 2020, pp. 1–8.